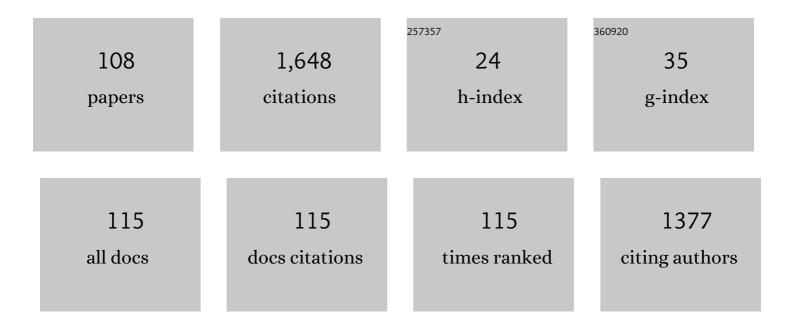
Satoshi Tanaka

List of Publications by Year in descending order

Source: https://exaly.com/author-pdf/5193053/publications.pdf Version: 2024-02-01



#	Article	IF	CITATIONS
1	Domain coarsening in viscous sintering as a result of topological pore evolution. Journal of the European Ceramic Society, 2022, 42, 729-733.	2.8	5
2	Direct observation of the deformation behavior of agglomerates in a highly concentrated slurry under startup shear flow. Open Ceramics, 2022, 9, 100209.	1.0	2
3	Hardening of (Ba _{0.5} Na _{0.5}) _{0.85} Ba _{0.15} TiO ₃ lead-free piezoelectric ceramics by adding (Bi _{0.5} Na _{0.5})MnO ₃ . Japanese lournal of Applied Physics. 2022. 61. SG1058.	0.8	4
4	Development of Functional Ceramics by Colloidal Processing in Rotating High Magnetic Field. Funtai Oyobi Fummatsu Yakin/Journal of the Japan Society of Powder and Powder Metallurgy, 2021, 68, 113-120.	0.1	1
5	Graded evolution of anisotropic microstructure during sintering from crystalâ€oriented powder compact. International Journal of Applied Ceramic Technology, 2020, 17, 677-684.	1.1	0
6	High-power properties of (Sr,Ca)2NaNb5O15piezoelectric ceramics in a longitudinal mode. Japanese Journal of Applied Physics, 2020, 59, SKKA07.	0.8	6
7	Fabrication of c-axis oriented hydroxyapatite ceramics in a rotating high magnetic field using photopolymerization. Journal of the European Ceramic Society, 2020, 40, 4332-4339.	2.8	9
8	Preparation and gas permeance of c-axis oriented zeolite membrane using ion-exchanged mordenite zeolite crystals oriented in magnetic field. Journal of the European Ceramic Society, 2020, 40, 5984-5990.	2.8	2
9	Effective oriented direction for enhancement of the piezoelectric properties of crystal-oriented (Li,) Tj ETQq1	0.784314	rgBŢ /Overlo
10	Defect formation and strength reliability during powder compaction and sintering process observed by Synchrotron X-ray CT. The Proceedings of the Materials and Processing Conference, 2020, 2020.28, 307.	0.0	0
11	Fabrication of Crystal-Oriented Bulk Piezoelectric Ceramics by Stereolithography in Magnetic Field. Funtai Oyobi Fummatsu Yakin/Journal of the Japan Society of Powder and Powder Metallurgy, 2020, 67, 621-628.	0.1	1
12	3D multiscale-imaging of processing-induced defects formed during sintering of hierarchical powder packings. Scientific Reports, 2019, 9, 11595.	1.6	27
13	Determination of sintering stress and bulk viscosity from sinter-forging and X-ray microtomography methods: a Review. Materials Today: Proceedings, 2019, 16, 42-48.	0.9	2
14	High-power properties of crystal-oriented (Sr,Ca) ₂ NaNb ₅ O ₁₅ piezoelectric ceramics and their application to ultrasonic motors. Japanese Journal of Applied Physics, 2019, 58, SGGA07.	0.8	9
15	Effects of ammonium molybdate additive and sintering temperature on the properties of foam ceramics based on ceramic tile polishing waste. Journal of the Ceramic Society of Japan, 2019, 127, 318-326.	0.5	4
16	[101]-Oriented (Li,Na,K) NbO ₃ ceramics prepared by magnetic field-assisted forming, sintering, and electric poling. Journal of the Ceramic Society of Japan, 2019, 127, 887-892.	0.5	3
17	Evaluation of Macroscopic Mechanical Properties from 3-D Visualization of Microstructure in Sintering. Funtai Oyobi Fummatsu Yakin/Journal of the Japan Society of Powder and Powder Metallurgy, 2019, 66, 604-610.	0.1	0
18	Influence of binder layer of spray-dried granules on occurrence and evolution of coarse defects in alumina ceramics during sintering. Journal of the European Ceramic Society, 2018, 38, 1846-1852.	2.8	15

#	Article	IF	CITATIONS
19	Particle Rotation in Colloidal Processing under a Strong Rotating Magnetic Field. Langmuir, 2018, 34, 6462-6469.	1.6	5
20	Influence of tetragonality on crystal orientation induced by a strong magnetic field and on the piezoelectric properties of the (Bi _{0.5} ,) Tj ETQq0 0 0 rgBT /Overlock 10 Tf 50 702 Td (Na <sub>0.5<!--</td--><td>sub>)<sub< td=""><td>>1â^'</td></sub<></td></sub> <	sub>) <sub< td=""><td>>1â^'</td></sub<>	>1â^'
	system. Journal of the Ceramic Society of Japan, 2018, 126, 655-661.		
21	Computation of sintering stress and bulk viscosity from microtomographic images in viscous sintering of glass particles. Journal of the American Ceramic Society, 2017, 100, 867-875.	1.9	20
22	Interface topology for distinguishing stages of sintering. Scientific Reports, 2017, 7, 11106.	1.6	41
23	Evaluation of Macroscopic Mechanical Properties from 3-D Visualization of Microstructure in Sintering. Funtai Oyobi Fummatsu Yakin/Journal of the Japan Society of Powder and Powder Metallurgy, 2017, 64, 495-500.	0.1	0
24	Effect of Slurry Temperature on Particle Orientation in Magnetic Field Assisted Forming Method. Journal of the Society of Powder Technology, Japan, 2016, 53, 791-796.	0.0	1
25	Complicated Flow Behavior of Silica Particles in Concentrated Slurry. Journal of the Society of Powder Technology, Japan, 2016, 53, 294-300.	0.0	1
26	Influence of granule characteristics on fabrication of translucent alumina ceramics with high strength and reliability. Journal of the Ceramic Society of Japan, 2016, 124, 426-431.	0.5	3
27	Colloidal processing using UV curable resin under high magnetic field for textured ceramics. Journal of the European Ceramic Society, 2016, 36, 2739-2743.	2.8	12
28	Stochastic analysis on ceramic granule collapse in powder compact during cold isostatic pressing. Advanced Powder Technology, 2016, 27, 940-947.	2.0	7
29	Fabrication of Transparent Grainâ€Oriented Polycrystalline Alumina by Colloidal Processing. Journal of the American Ceramic Society, 2016, 99, 3217-3219.	1.9	18
30	Particle sedimentation monitoring in high-concentration slurries. AIP Advances, 2016, 6, .	0.6	14
31	Coarse pore evolution in dry-pressed alumina ceramics during sintering. Advanced Powder Technology, 2016, 27, 1006-1012.	2.0	31
	Crystal-oriented (Bi _{0.5} ,) Tj ETQq0 0 0 rgBT /Overlock 10 Tf 50 232 Td (Na _{0.58}	<td>;)<sub>< td=""></sub><></td>	;) <sub>< td=""></sub><>
32	ceramics prepared by colloidal processing in rotating high magnetic field. Journal of the Ceramic	0.5	9
33	Society of Japan, 2015, 123, 340-344. Stress Estimation for Multiphase Ceramics Laminates During Sintering. Ceramic Engineering and Science Proceedings, 2015, , 101-106.	0.1	0
34	Observation of Particle Motion in High oncentration Ceramic Slurries Under Low Shear Rate. Journal of the American Ceramic Society, 2015, 98, 1429-1436.	1.9	5
35	Fabrication of transparent crystal-oriented polycrystalline strontium barium niobate ceramics for electro-optical application. Journal of the European Ceramic Society, 2014, 34, 3723-3728.	2.8	26
36	Elastic Analysis on Homogenization Process in Ceramic Powder Compact during Repeated Cold Isostatic Pressing by Multiple Shell Model. Journal of the Society of Powder Technology, Japan, 2014, 51, 153-162.	0.0	1

#	Article	IF	CITATIONS
37	Enhancing the contrast of low-density packing regions in images of ceramic powder compacts using a contrast agent for micro-X-ray computed tomography. Journal of the Ceramic Society of Japan, 2014, 122, 574-576.	0.5	6
38	Influence of Aggregates in αâ€ <scp><scp>Al</scp></scp> ₂ <scp><scp>O</scp></scp> ₃ Slurry on Orientation Degree of Powder Compact Fabricated by Magnetic Forming Method. Journal of the American Ceramic Society, 2013, 96, 2411-2418.	1.9	3
39	Thermal anisotropy of epoxy resin-based nano-hybrid films containing BN nanosheets under a rotating superconducting magnetic field. Materials Chemistry and Physics, 2013, 139, 355-359.	2.0	15
40	Controlled Linear Assemblies of Graphite Flakes Anchoring Polysiloxane-Based Nanocomposite Films and Enhancement of Thermal Properties. Japanese Journal of Applied Physics, 2013, 52, 028005.	0.8	0
41	Densely Packed Linear Assembles of Carbon Nanotube Bundles in Polysiloxane-Based Nanocomposite Films. Journal of Nanomaterials, 2013, 2013, 1-10.	1.5	9
42	Anisotropic sintering behavior of grain-oriented strontium barium niobate ceramics. Journal of the Ceramic Society of Japan, 2013, 121, 411-415.	0.5	5
43	High-Power Piezoelectric Characteristics of C-Axis Crystal-Oriented (Sr,Ca) ₂ NaNb ₅ O ₁₅ Ceramics. Japanese Journal of Applied Physics, 2012, 51, 09LD02.	0.8	9
44	Evaluation of dispersability of gamma alumina prepared by homogeneous precipitation. Journal of the Ceramic Society of Japan, 2012, 120, 290-294.	0.5	9
45	Electric-field-assisted fabrication of linearly stretched bundles of microdiamonds in polysiloxane-based composite material. Diamond and Related Materials, 2012, 26, 7-14.	1.8	13
46	Polyepoxide-based nanohybrid films with self-assembled linear assemblies of nanodiamonds. Acta Materialia, 2012, 60, 7249-7257.	3.8	5
47	Quantitative analysis of de-aggregation behavior in alumina suspension by beads milling. Powder Technology, 2012, 217, 619-623.	2.1	4
48	High-Power Piezoelectric Characteristics of <i>C</i> -Axis Crystal-Oriented (Sr,Ca) ₂ NaNb ₅ O ₁₅ Ceramics. Japanese Journal of Applied Physics, 2012, 51, 09LD02.	0.8	6
49	Anisotropic sintering of oriented ceramics prepared in a rotating magnetic field. IOP Conference Series: Materials Science and Engineering, 2011, 21, 012008.	0.3	0
50	Fabrication of highly particle-oriented alumina green compact from non-aqueous slurry. Journal of the Ceramic Society of Japan, 2011, 119, 198-202.	0.5	6
51	Compatibility of PVB of Mixed Organic Solvents in Alumina Slurries and its Effect on Morphology of Green Sheets. Journal of the American Ceramic Society, 2011, 94, 2819-2824.	1.9	4
52	Microstructural Evidence of Hall Mobility Anisotropy in c-Axis Textured Al-Doped ZnO. Journal of the American Ceramic Society, 2011, 94, 2339-2343.	1.9	19
53	Epoxy resin-based nanocomposite films with highly oriented BN nanosheets prepared using a nanosecond-pulse electric field. Materials Letters, 2011, 65, 2426-2428.	1.3	28
54	Self-assemblies of linearly aligned diamond fillers in polysiloxane/diamond composite films with enhanced thermal conductivity. Composites Science and Technology, 2011, 72, 112-118.	3.8	49

Satoshi Tanaka

#	Article	IF	CITATIONS
55	Facile orientation of unmodified BN nanosheets in polysiloxane/BN composite films using a high magnetic field. Journal of Materials Science, 2011, 46, 2318-2323.	1.7	27
56	Modification of BN nanosheets and their thermal conducting properties in nanocomposite film with polysiloxane according to the orientation of BN. Composites Science and Technology, 2011, 71, 1046-1052.	3.8	105
57	Formation and Structural Characteristic of Perpendicularly Aligned Boron Nitride Nanosheet Bridges in Polymer/Boron Nitride Composite Film and Its Thermal Conductivity. Japanese Journal of Applied Physics, 2011, 50, 01BJ05.	0.8	8
58	Linear Assembles of BN Nanosheets, Fabricated in Polymer/BN Nanosheet Composite Film. Journal of Nanomaterials, 2011, 2011, 1-7.	1.5	30
59	Formation and Structural Characteristic of Perpendicularly Aligned Boron Nitride Nanosheet Bridges in Polymer/Boron Nitride Composite Film and Its Thermal Conductivity. Japanese Journal of Applied Physics, 2011, 50, 01BJ05.	0.8	4
60	Orientation distribution-Lotgering factor relationship in a polycrystalline material-as an example of bismuth titanate prepared by a magnetic field. Journal of the Ceramic Society of Japan, 2010, 118, 921-926.	0.5	84
61	Fabrication of c-axis-oriented potassium strontium niobate (KSr2Nb5O15) ceramics by a rotating magnetic field and electrical property. Journal of the Ceramic Society of Japan, 2010, 118, 722-725.	0.5	18
62	Facile preparation of a polysiloxane-based hybrid composite with highly-oriented boron nitride nanosheets and an unmodified surface. Composites Science and Technology, 2010, 70, 1681-1686.	3.8	59
63	Strengthâ€Processing Defects Relationship Based on Micrographic Analysis and Fracture Mechanics in Alumina Ceramics. Journal of the American Ceramic Society, 2009, 92, 688-693.	1.9	34
64	c-axis oriented ZnO formed in a rotating magnetic field with various rotation speeds. Journal of the European Ceramic Society, 2009, 29, 955-959.	2.8	25
65	Effect of polyacrylic acid (PAA) binder system on particle orientation during dry-pressing. Powder Technology, 2009, 196, 133-138.	2.1	8
66	Fabrication of crystal-oriented barium-bismuth titanate ceramics in high magnetic field and subsequent reaction sintering. Science and Technology of Advanced Materials, 2009, 10, 014602.	2.8	16
67	Estimation of Weibull modulus from coarser defect distribution in dry-pressed alumina ceramics. Journal of the Ceramic Society of Japan, 2009, 117, 742-747.	0.5	14
68	The effect of packing structure of powder particles on warping during sintering. Journal of the European Ceramic Society, 2008, 28, 21-25.	2.8	10
69	Evolution of Discontinuity in Particle Orientation in Ceramic Tape Casting. Journal of the American Ceramic Society, 2008, 91, 3181-3184.	1.9	9
70	Effect of Segregation of a Polyacrylic Acid (PAA) Binder on the Green Strength of Dryâ€Pressed Alumina Compacts. Journal of the American Ceramic Society, 2008, 91, 3896-3902.	1.9	8
71	C-axis-Oriented (Sr,Ca) ₂ NaNb ₅ O ₁₅ Multilayer Piezoelectric Ceramics Fabricated Using High-Magnetic-Field Method. Japanese Journal of Applied Physics, 2008, 47, 7693.	0.8	22
72	Zinc Oxide Ceramics with High Mobility as n-Type Thermoelectric Materials. Materials Science Forum, 2007, 561-565, 581-586.	0.3	1

SATOSHI TANAKA

#	Article	IF	CITATIONS
73	Fabrication of <i>c</i> -axis oriented higher manganese silicide by a high-magnetic-field and its thermoelectric properties. Journal of Materials Research, 2007, 22, 2917-2923.	1.2	19
74	Development of Packing Structure of Powder Particles in Tape Casting. Journal of the Ceramic Society of Japan, 2007, 115, 136-140.	1.3	7
75	Particle Oriented Strontium Bismuth Titanate Ceramics Prepared by Using High Magnetic Field and Subsequent Reaction Sintering. Journal of the Ceramic Society of Japan, 2007, 115, 237-240.	1.3	20
76	Orientation dependence of transport property and microstructural characterization of Al-doped ZnO ceramics. Acta Materialia, 2007, 55, 4753-4757.	3.8	49
77	A quantitative evaluation method for particle orientation structure in alumina powder compacts. Journal of the European Ceramic Society, 2007, 27, 3399-3406.	2.8	17
78	Packing Structure of Particles in a Green Compact and Its Influence on Sintering Deformation. Journal of the American Ceramic Society, 2007, 90, 3717-3719.	1.9	12
79	C-Axis Orientation of KSr2Nb5O15Using a Rotating Magnetic Field. Journal of the American Ceramic Society, 2007, 90, 3503-3506.	1.9	39
80	Effect of internal binder on microstructure in compacts made from granules. Journal of the European Ceramic Society, 2007, 27, 873-877.	2.8	28
81	Fabrication of c-axis Oriented Zn0.98Al0.02O by a High-Magnetic-Field via Gelcasting and its Thermoelectric Properties. Journal of the Ceramic Society of Japan, 2006, 114, 1085-1088.	1.3	34
82	Design of Packing Structures through Direct Characterization of Ceramics Green Bodies. Journal of the Ceramic Society of Japan, 2006, 114, 141-146.	1.3	6
83	Effect of Organic Binder Segregation on Sintered Strength of Dry-Pressed Alumina. Journal of the American Ceramic Society, 2006, 89, 1903-1907.	1.9	31
84	Observation of the granule packing structure using a confocal laser-scanning microscope. Journal of the European Ceramic Society, 2006, 26, 683-687.	2.8	4
85	Crystal-Oriented La-Substituted Sr2NaNb5O15Ceramics Fabricated Using High-Magnetic-Field Method. Japanese Journal of Applied Physics, 2006, 45, 7460-7464.	0.8	23
86	Improvement of Second-Order Optical Nonlinearity in Transparent Ba ₂ TiGe ₂ O ₈ Crystallized Glasses Prepared in High Magnetic Field. Advanced Materials Research, 2006, 11-12, 193-196.	0.3	1
87	Preparation and Thermoelectric Property of Highly Oriented Al-Doped ZnO Ceramics by a High Magnetic Field. Japanese Journal of Applied Physics, 2006, 45, L1212-L1214.	0.8	30
88	Fabrication of c-axis oriented polycrystalline ZnO by using a rotating magnetic field and following sintering. Journal of Materials Research, 2006, 21, 703-707.	1.2	62
89	Evaluation of Bubble Content in Aqueous Alumina Slurries. Journal of the Ceramic Society of Japan, 2005, 113, 449-451.	1.3	2
90	Characterization of Internal Structure of a Green Body Made by Dry-Pressing. Key Engineering Materials, 2004, 264-268, 189-192.	0.4	2

SATOSHI TANAKA

#	Article	IF	CITATIONS
91	Crystal-Oriented Bi4Ti3O12Ceramics Fabricated by High-Magnetic-Field Method. Japanese Journal of Applied Physics, 2004, 43, 6645-6648.	0.8	36
92	Infrared Microscopy as a Powerful Tool for the Examination of Internal Microstructure of Nano-Powder Compact-Yittria Stabilized Zirconia as a Model Journal of the Ceramic Society of Japan, 2004, 112, 114-116.	1.3	5
93	Particle Orientation Distribution in Alumina Compact Body Prepared by the Slip Casting Method. Journal of the Ceramic Society of Japan, 2004, 112, 276-279.	1.3	18
94	Influence of Dehydration Rate on the Degree of Particle Orientation in Alumina Green Body Made by Slip Casting. Journal of the Ceramic Society of Japan, 2004, 112, 641-645.	1.3	4
95	Direct observation of aggregates and agglomerates in alumina granules. Powder Technology, 2003, 129, 153-155.	2.1	16
96	Morphological Change of Large Pores in Alumina Ceramics in the Final Stage of Densification. Journal of the Ceramic Society of Japan, 2003, 111, 525-527.	1.3	6
97	Particle Oriented Bismuth Titanate Ceramics Made in High Magnetic Field. Journal of the Ceramic Society of Japan, 2003, 111, 702-704.	1.3	72
98	Grain Oriented Microstructure Made in High Magnetic Field. Key Engineering Materials, 2002, 206-213, 445-448.	0.4	24
99	New characterization method for pore and packing structure in powder compacts using confocal laser scanning microscope. Journal of Electron Microscopy, 2002, 51, 215-223.	0.9	1
100	Effect of Cold Isostatic Pressing on Microstructure and Shrinkage Anisotropy during Sintering of Uniaxially Pressed Alumina Compacts Journal of the Ceramic Society of Japan, 2002, 110, 264-269.	1.3	15
101	Sintering deformation caused by particle orientation in uniaxially and isostatically pressed alumina compacts. Journal of the European Ceramic Society, 2002, 22, 311-316.	2.8	43
102	Kinetics of property change associated with atmospheric humidity changes in alumina powder granules with PVA binder. Journal of the European Ceramic Society, 2002, 22, 2835-2840.	2.8	20
103	Fractography for Alumina Ceramics Using a Confocal Scanning Laser Microscope Journal of the Ceramic Society of Japan, 2001, 109, 1055-1056.	1.3	1
104	Infrared Microscopy for Examination of Structure in Sprayâ€Dried Granules and Compacts. Journal of the American Ceramic Society, 2001, 84, 254-256.	1.9	18
105	Direct Evidence for Lowâ€Density Regions in Compacted Sprayâ€Dried Powders. Journal of the American Ceramic Society, 2001, 84, 2454-2456.	1.9	14
106	Piezoelectric Properties of <i>c</i> -Axis-Oriented (Sr,Ca) ₂ NaNb ₅ O ₁₅ Piezoelectric Ceramics with Single-Plate Type and Multilayered Type Fabricated Using Crystal-Oriented Sheet Forming. Key Engineering Materials, 0, 421-422, 21-25.	0.4	3
107	Linear Assembly of Oxidized Surface Treated Nanodiamonds in Polymer-Based Nanohybrids by Electric Field Inducement. Materials Science Forum, 0, 761, 107-111.	0.3	0
108	Anisotropic Properties of Al Doped ZnO Ceramics Fabricated by the High Magnetic Field. , 0, , 113-120.		0